

See discussions, stats, and author profiles for this publication at:  
<https://www.researchgate.net/publication/229421934>

# Rydberg states of acetylene clusters (C<sub>2</sub>H<sub>2</sub>)<sub>2</sub> and (C<sub>2</sub>H<sub>2</sub>)<sub>3</sub> resolved by two- photon resonant ionization spectroscopy

ARTICLE *in* CHEMICAL PHYSICS LETTERS · JULY 1994

Impact Factor: 1.9 · DOI: 10.1016/0009-2614(94)00529-X

---

CITATIONS

10

---

READS

10

5 AUTHORS, INCLUDING:



[Steve Allman](#)

Oak Ridge National Laboratory

85 PUBLICATIONS 1,466 CITATIONS

SEE PROFILE



[W. R. Garrett](#)

University of Tennessee

166 PUBLICATIONS 2,334 CITATIONS

SEE PROFILE



ELSEVIER

8 July 1994

Chemical Physics Letters 224 (1994) 7-15

**CHEMICAL  
PHYSICS  
LETTERS**

## Rydberg states of acetylene clusters $(C_2H_2)_2$ and $(C_2H_2)_3$ resolved by two-photon resonant ionization spectroscopy

Y.F. Zhu, S.L. Allman, R.C. Phillips, W.R. Garrett, C.H. Chen \*

*Oak Ridge National Laboratory, P.O. Box 2008, Bldg 5500, MS-6378, Oak Ridge, TN 37831, USA*

Received 4 March 1994; in final form 2 May 1994

### Abstract

The Rydberg states of the acetylene clusters  $(C_2H_2)_2$  and  $(C_2H_2)_3$  have been resolved by the technique of two-photon resonant ionization spectroscopy in the energy region of the monomer gerade Rydberg states. The stability of these cluster Rydberg states has been found to be vibrational mode dependent. The geometry of the clusters, and the mechanism of the dissociative ionization have been discussed.

### 1. Introduction

The recent progress of intracluster ion-molecule reactions [1-16] in cluster ion chemistry has received more attention due to its distinct features, such as the reaction collision from fixed orientation, small impact parameters and zero collision energy. In this approach, the transition state of the collision complex and the mechanism of the ion-molecule reaction can be better understood than from studies applying the conventional ion-molecule reaction. The unimolecular decomposition of some homogenous cluster ions such as  $(NH_3)_n^+$  [1-3,12],  $(C_2H_2)_n^+$  [13-15],  $(C_2H_4)_n^+$  [8],  $(H_2O)_n^+$  [5,6],  $(C_6H_6)_n^+$  [7,16],  $(CH_3X)_n^+$  [9,10], and  $(NO_2)_n^+$  [4] have been investigated by electron impact ionization or VUV photoionization mass spectrometry. Among these clusters  $(C_2H_2)_n^+$  is the most important one because of its simple bonding in clusters and the several possible channels for ion-molecule reactions, thus it can serve as an excellent prototype candidate

for study of cluster ionization and dissociation.

By applying VUV photoionization of neutral acetylene clusters and mass detection of the fragment ions, Ono and Ng [13] discovered that the appearance energies for  $C_4H_3^+$  and  $C_4H_2^+$  from  $(C_2H_2)_2$  were  $10.90 \pm 0.05$  eV ( $1137 \pm 5$  Å), which suggest activation energies of  $\approx 0$  and  $\approx 12$  kcal/mol for the  $C_4H_3^+ + H$  and the  $C_4H_2^+ + H_2$  reaction channels, respectively. Their result also reveals evidence that the high vibrationally excited levels of the  $X^2\Pi_u$  state are as effective as the  $A^2\Sigma_g^+$  state in the formation of  $C_4H_2^+ + 2H$ . In addition to the observed fragment ions by using the near-threshold photoionization method, Shinohara and his co-workers [8] found intact cluster ions of acetylene  $(C_2H_2)_n^+$  ( $n=2-4$ ), which have not been detected in the (full-collision) conventional ion-molecule reactions of acetylene. The observation of these intact clusters has been ascribed to the effect that the excess energies on ionization are randomized within the ionized clusters  $[(Ar)_n(C_2H_2)_m]^+$  and finally converted to the ejection of Ar atoms. Using the threshold photoelectron-photoion coincidence technique, Booze and Baer

\* Corresponding author.

[15] have observed the dissociative ionization of the acetylene clusters as the only pathways, and no direct ionization of  $(\text{C}_2\text{H}_2)_2$ ,  $(\text{C}_2\text{H}_2)_3$  and  $(\text{C}_2\text{H}_2)_4$  to the stable ions  $\text{C}_4\text{H}_4^+$ ,  $\text{C}_6\text{H}_6^+$ , and  $\text{C}_8\text{H}_8^+$  for the photon energies between 10.20 and 11.27 eV. The shapes of the time of flight peaks in their spectra indicate that the fragmentation of the acetylene cluster fits into the statistical dissociation dynamics, and the neutral T-shaped dimer and triangular trimer geometries are unstable on the ionic potential energy surface. Those research achievements have greatly extended the knowledge of the ion–molecule reactions. However, many questions with respect to the transition state of the collision complex and the reaction mechanism are left unaddressed. For instance, are there stable geometries for  $(\text{C}_2\text{H}_2)_2^+$  and  $(\text{C}_2\text{H}_2)_3^+$  clusters? Is the mechanism of the intracluster ion–molecule reaction controllable by the optical selection of the electronic and vibrational states of the monomer unit inside of cluster? To what degree does the intermolecular reaction compete with the stabilization via monomer evaporation?

In the studies outlined above, the results of the intracluster ion–molecule reaction show the distributions of the fragment ions in the fashion of statistical equilibrium. However, the results of neutral cluster photodissociation [17–19] present evidence that the dissociation of weakly bound clusters could be mode specific. It is seen that the statistical results of fragmentation from the cluster ions in the above experiments could be induced by the one-photon direct ionization scheme. The geometry of  $(\text{C}_2\text{H}_2)_n^+$  clusters is subject to a large change upon the ionization from neutral clusters. The geometry difference between the ion and the neutral clusters introduces the non-adiabatic excitation effect for the one-photon ionization, i.e. the broad population distributions of the cluster ions in the vibrational modes. The fragmentation and the dissociation (or monomer evaporation) from these cluster ions naturally fall into the statistical model. Thus the state selection of the dimer and trimer ions becomes the key step for the study of the intracluster ion–molecule reaction dynamics. Such state selection can be effectively achieved only through the optical excitation of Rydberg states of the clusters, in which the ejection of a Rydberg electron from the intermediate state is considered to be an adiabatic process. This follows from the fact that the

potential energy surface of the cluster ion and the neutral cluster with a Rydberg excitation are virtually identical.

In clusters, the vibrational frequencies associated with intermolecular motion are considerably lower than the intramolecular modes. Any coupling between the intermolecular motion and the intramolecular one will result in the dissociation of clusters during the optical excitation. Therefore it is very difficult to spectroscopically resolve the Rydberg states of clusters with a polyatomic monomer. Most of the Rydberg states of clusters are unstable except the one with a small change both in the geometry and the dipole moment compared to the ground state. Fortunately, the gerade Rydberg states of the  $\text{C}_2\text{H}_2$  molecule fall into this category. In this study, we present results of the Rydberg states of  $(\text{C}_2\text{H}_2)_2$  and  $(\text{C}_2\text{H}_2)_3$  clusters using a two-photon resonant ionization spectroscopy method. Results indicate that the  $(\text{C}_2\text{H}_2)_2^+$  and  $(\text{C}_2\text{H}_2)_3^+$  could be stable upon adiabatic ionization from a Rydberg state. The stability of these ions is vibrational mode dependent, and the state selection of these cluster ions is possible.

## 2. Experimental

Resonant multiphoton ionization spectroscopy was conducted in a high-vacuum chamber equipped with a quadrupole mass spectrometer (QUAD 1110A) and a pulsed supersonic jet (Lasertechnics model 203). The experimental setup is illustrated in Fig. 1. Gas mixtures of different acetylene concentrations were used for the supersonic cooling. The molecular beam nozzle has an orifice diameter of 0.3 mm. The background pressure in the vacuum chamber was kept around  $2.0 \times 10^{-5}$  Torr with 500 Torr stagnation pressure of the gas mixture during the experiment. Because the higher-order acetylene cluster ions can lose one or more monomer units by evaporation, the resonant ionization spectra may contain contributions from the higher-order clusters. In order to avoid this contamination, acetylene concentrations of 0.2%, 7% and 70% were used for the two-photon resonant ionization of  $\text{C}_2\text{H}_2$ ,  $(\text{C}_2\text{H}_2)_2$  and  $(\text{C}_2\text{H}_2)_3$ , respectively. At these relatively low acetylene concentrations the density of the higher-order acetylene clusters is negligible, e.g. with an acetylene concentration

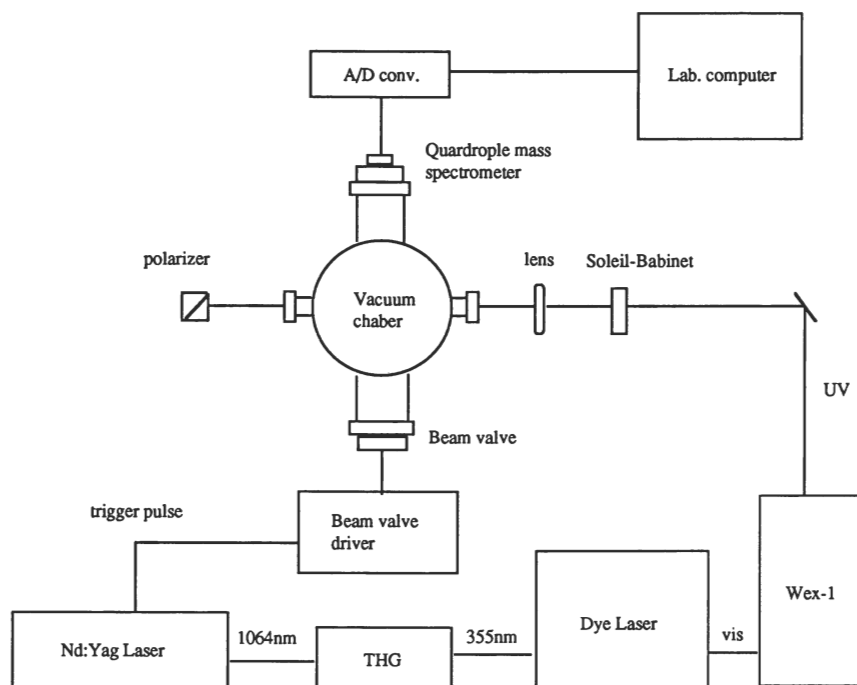


Fig. 1. Diagram of experimental setup.

of 0.2% the density of acetylene dimer will be very low compared to the monomer, and the  $(C_2H_2)_2^+$  signal is below the detection limit. So the contributions of  $C_2H_2^+$  signal from the evaporation of dimer ions can be neglected. These limiting conditions also have been found in Ono and Ng's experiment [13]. In the present experiment we have not found a detectable signal of  $(C_2H_2 \cdot Ar_n)^+$  ions, which indicates the unstable character of the Rydberg states of the acetylene–argon clusters. Therefore there is no experimental evidence for the  $(C_2H_2)_n^+$  ion signal from the acetylene–argon cluster channels. The dc field for the ion collection may introduce the perturbation for Rydberg states of the acetylene clusters, which then destabilize the Rydberg state of acetylene clusters. For the purpose of avoiding such perturbations the dc voltage for the ion collection has been kept to a low limit of 7 V/cm during the experiment. We note that expansion using He as the carrier gas can provide a deeper cooling effect than argon gas. However, controlling the density of acetylene clusters in He becomes difficult. The argon gas used in the experiment is the UHP grade (Air Liquid Co product). The

source of acetylene used is 99.6% purity gas from Matheson.

The two-photon transition by linear/circular polarized light was performed in the following way. A Soleil-Babinet Compensator (special optics) was installed in the laser path before the focusing lens for generating linear/circular polarized light. A polarizer was installed after the exit entrance of the vacuum chamber to determine the polarization of the laser beam. Over a short wavelength region (1 nm), the Soleil-Babinet Compensator can generate good quality linear/circular polarized light. The residual linearly polarized light in the circularly polarized beam are estimated to be less than 5.0%. The spectra of the two-photon transition by linear polarized excitation was recorded first. Then the micrometer of the Soleil-Babinet Compensator was tuned to the position for generating circular polarized light without changing other experimental conditions, and the spectra of two-photon transition by circular polarized excitation was recorded afterwards. By this technique, we avoid the problems of the laser energy deviations and the displacement of focus position of the linear/circular po-

larized laser beam using a Fresnel rhomb as an achromatic circular polarizer.

The frequency-doubled output ( $\approx 1$  mJ/pulse in the 264–271 nm region obtained by Spectra-Physics WEX-1) of a pulsed dye laser (Spectra-Physics PDL-2 with the bandwidth of  $0.3\text{ cm}^{-1}$ ) pumped by the frequency-doubled output of a Nd:YAG laser (Quanta Ray DCR-2A) operated at 10 Hz was focused (f.l. 35 cm) onto a point 40 mm downstream from the nozzle exit. Two-photon resonant ionization spectra were collected by scanning the laser wavelength of the dye laser while observing the ion signal of  $\text{C}_2\text{H}_2^+$  (mass 26),  $(\text{C}_2\text{H}_2)_2^+$  (mass 52) and  $(\text{C}_2\text{H}_2)_3^+$  (mass 78) ion channels.

The pulsed ion signal from the channeltron was digitized by Metrabyte's A/D converter which was installed in an IBM lab computer, and was averaged over 10 laser shots. The laser wavelength of the spectra was calibrated by the Ne atomic transitions and converted into the vacuum wavelength units of  $\text{cm}^{-1}$ .

### 3. Results

A two-photon resonant ionization spectrum of the  $\text{C}_2\text{H}_2$  monomer Rydberg state is shown in Fig. 2. Trace (a) in Fig. 2 represents the two-photon gerade–gerade transition of the acetylene monomer,

which was resolved by Ashfold and co-workers [20]. Traces (b) and (c) in Fig. 2 show the two-photon transitions of the acetylene  $(\text{C}_2\text{H}_2)_2$  dimer and  $(\text{C}_2\text{H}_2)_3$  trimer, respectively. The energy diagram for this transition is shown in Fig. 3. Fig. 4 represents the two-photon spectra of the  $\text{C}_2\text{H}_2$  monomer for the origin of the  $^1\Delta_g$  Rydberg electronic state by the linear/circular polarized excitation. The upper trace in Fig. 4 is the spectrum obtained by linearly polarized excitation while the bottom trace is the spectrum obtained by circularly polarized excitation. Fig. 5 gives the two-photon spectrum of the  $(\text{C}_2\text{H}_2)_2$  dimer for the origin of the  $^1\Delta_g$  Rydberg electronic state by the linear/circular polarized excitation. The upper trace is for the linearly polarized excitation and the bottom trace is for the circularly polarized excitation. Due to the different acetylene concentrations used in the experiment, we did not intend to normalize the transition intensity between monomer and clusters. Therefore the relative distributions of the monomer and cluster density under our expansion condition have not been obtained. The transition intensities at different wavelength region in Fig. 2 have been normalized based on the laser power. Listed in Table 1 are all the resolved energy positions for the Rydberg transitions of  $\text{C}_2\text{H}_2$ ,  $(\text{C}_2\text{H}_2)_2$  and  $(\text{C}_2\text{H}_2)_3$ .

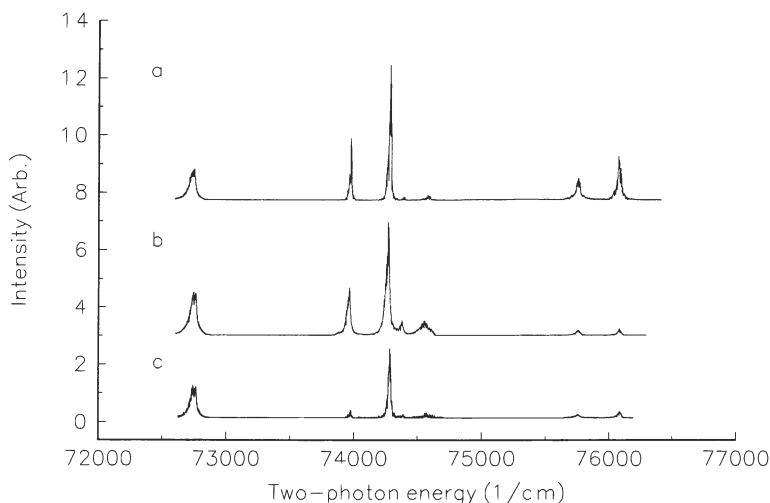


Fig. 2. Two-photon resonant ionization spectra of  $\text{C}_2\text{H}_2$  molecule. The horizontal axis represents the total energy of two-photon transition in  $\text{cm}^{-1}$  and the vertical axis represents the  $\text{C}_2\text{H}_2^+$  signal in arbitrary units. (a), (b), and (c) represent the spectra of monomer, dimer, and trimer, respectively. The assignments of these peaks are listed in Table 1.

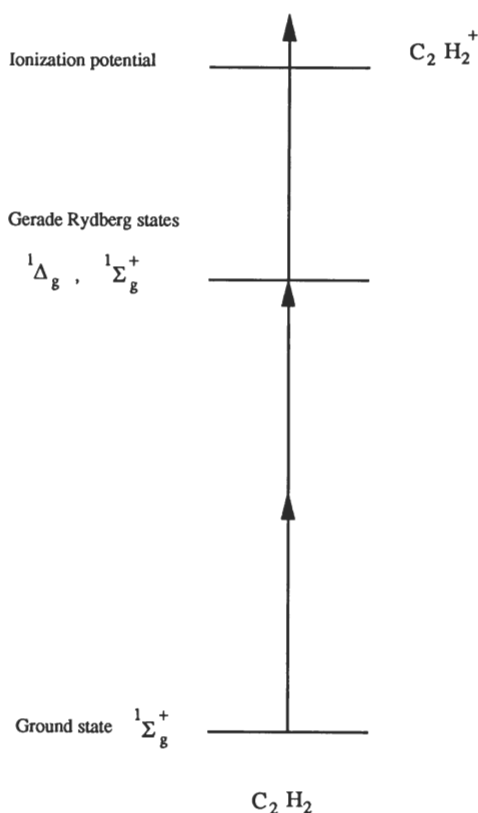


Fig. 3. Energy diagram of acetylene two-photon Rydberg transitions.

## 4. Discussion

### 4.1. Gerade Rydberg state of $C_2H_2$ and its clusters

The gerade Rydberg states of the acetylene molecule arise from promoting a  $\pi_u$  bonding electron to the  $3p_u$  Rydberg orbital. The angular momentum coupling of the ion core and the Rydberg electron result in  $\Delta_g$ ,  $\Pi_g$  and  $\Sigma_g^\pm$  electronic states. In one-color two-photon transitions the  $\Pi_g \leftarrow \Sigma_g^+$  and  $\Sigma_g^- \leftarrow \Sigma_g^+$  transitions are forbidden. The singlet  $\Delta_g$  and  $\Sigma_g^+$  states have been experimentally resolved [20] by two-photon resonant ionization spectroscopy based on the g–g symmetry selection rule. The origin of  $\Delta_g$  and  $\Sigma_g^+$  electronic states were assigned to the peaks at 72753 and 74286  $\text{cm}^{-1}$ , respectively. The  $\Delta_g \leftarrow \Sigma_g^+$  two-photon transition is controlled by the second rank component  $T_2^2$  of the transition tensor, which results in five branches with the dominant  $^S S$  and  $^S R$  branches. Since many rotational transitions overlap each other, the polarization effect of these branches can be well described by the classical orientation average, which gives an intensity ratio of 2/3 for the linear/circular polarized excitation [21]. The intensity ratio of the linear/circular polarized excitation for  $\Delta_g \leftarrow \Sigma_g^+$  transition in our spectra (shown in Fig. 4) have a value of  $0.59 \pm 0.04$ , which is very close to theoretical value of 0.67. This result indicates that the  $\Delta_g$  origin was

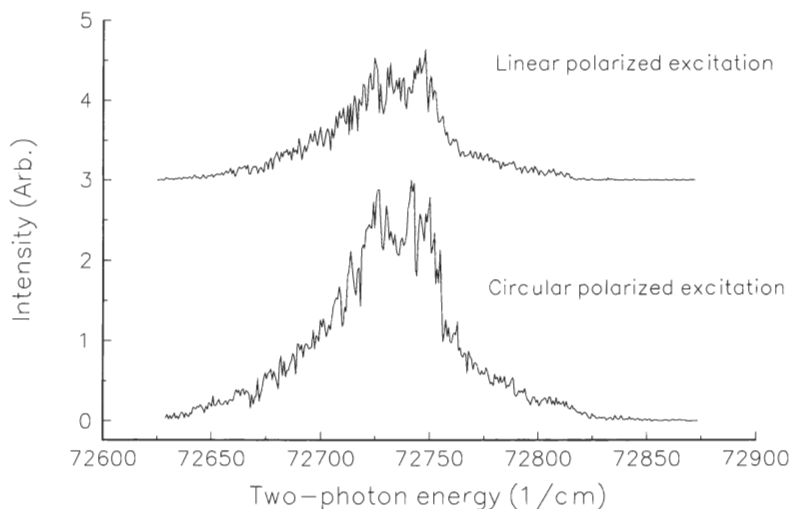


Fig. 4. Spectra of the polarization effect for the origin of the  $C_2H_2$   $1\Delta_g$  electronic state. The horizontal axis represents the total energy of the two-photon transition in  $\text{cm}^{-1}$  and the vertical axis represents the  $C_2H_2^+$  signal in arbitrary units.

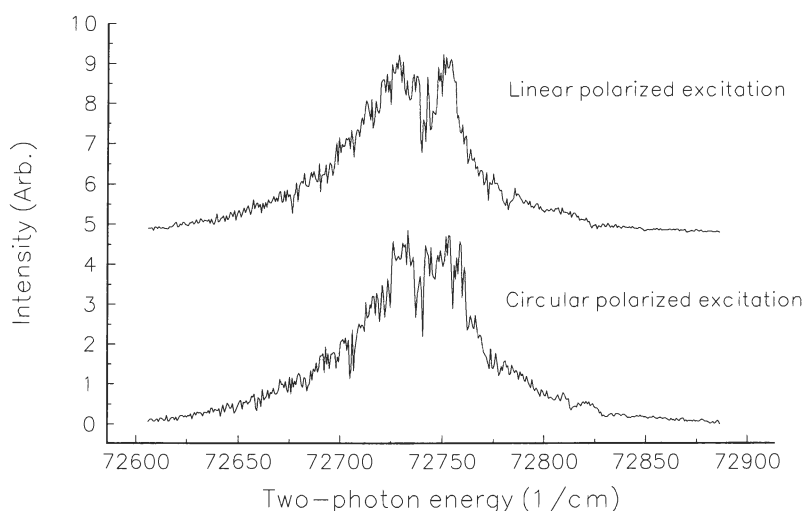


Fig. 5. The spectra of the polarization effect for the origin of the  $(\text{C}_2\text{H}_2)_2$   $^1\Delta_g$  electronic state. The horizontal axis represents the total energy of the two-photon transition in  $\text{cm}^{-1}$  and the vertical axis represents the  $(\text{C}_2\text{H}_2)_2^+$  signal in arbitrary units.

Table 1

The energy positions ( $\text{cm}^{-1}$ ) and vibronic symmetry of the two-photon Rydberg transitions for  $\text{C}_2\text{H}_2$ ,  $(\text{C}_2\text{H}_2)_2$  and  $(\text{C}_2\text{H}_2)_3$

Rydberg states	Vibronic symmetry	$\text{C}_2\text{H}_2$	$(\text{C}_2\text{H}_2)_2$	$(\text{C}_2\text{H}_2)_3$
$^1\Delta_g$ $0_0^0$	$\Delta_g$	72740	72743	72740
$^1\Delta_g$ $4_0^0$	$\Sigma_g^+$	73963	73962	73958
$^1\Sigma_g^+$ $0_0^0$	$\Sigma_g^+$	74274	74274	74272
$^1\Delta_g$ $5_0^0$	$\Sigma_g^+$	74388	74383	74377
$^1\Delta_g$ $2_0^1$	$\Delta_g$	74575	74558	74558
$^1\Delta_g$ $2_0^1 4_0^0$	$\Sigma_g^+$	75761	75764	75766
$^1\Sigma_g^+$ $2_0^1$	$\Sigma_g^+$	76086	76082	76079

correctly assigned. The spectrum of the  $\Delta_g$  state with a high-resolution scan (Fig. 4) shows a doublet feature. This doublet may belong to the strong  $^{\text{S}}\text{S}$  and  $^{\text{S}}\text{R}$  branches of  $\Delta_g \leftarrow \Sigma_g^+$  transition.

The  $\Sigma_g^+ \leftarrow \Sigma_g^+$  two-photon transition is controlled by the zeroth rank  $T_0^0$  and the second rank  $T_2^0$  component of the transition tensor. With the circularly polarized excitation, the  $T_0^0$  component becomes zero while the contribution from the  $T_2^0$  component is enhanced by a factor of  $\frac{3}{2}$  for the same light intensity. Therefore the intensity ratio of linear/circular polarized excitation is generally larger than 1 because of the dominant  $^{\text{Q}}\text{Q}$  branch in this transition. Our results also confirm the correct assignment of the origin of the  $\Sigma_g^+$  Rydberg state. The bending vibrational

assignment is less clear since numerous vibronic interactions and perturbations are conceivable in this region of the vertical electronic spectrum of acetylene, once bending vibrations are considered to be active. Therefore the strong transition at the position of  $73963 \text{ cm}^{-1}$  was assigned [20] to  $\nu=2$  for the bending vibration of either  $\nu_4$  (trans-bending) or  $\nu_5$  (cis-bending) mode. The coupling of the electronic angular momentum ( $A=2$ ) and the vibrational angular momentum ( $l=2$ ) give the  $\Delta_g$ ,  $\Sigma_g^\pm$  and  $\Gamma_g$  vibronic states. From the effect of the linear/circular polarized excitation, the transition positioned at  $73963 \text{ cm}^{-1}$  has the symmetry of  $\Sigma_g^+$ . Based on the vibrational frequencies of  $\nu_4$  and  $\nu_5$  in the ground state and the other Rydberg states, this transition should be  $\Sigma_g^+$  component of  $\nu_4$  mode. The weak transition at  $74388 \text{ cm}^{-1}$  that remains unassigned in Ashfold's work also has the symmetry of  $\Sigma_g^+$ . It could be the  $\Sigma_g^+$  component of  $\nu_5$  vibrational mode. The vibrational progression of the  $\text{C}\equiv\text{C}$  stretching mode  $\nu_2$  is well resolved and analyzed.

The Rydberg transitions of  $(\text{C}_2\text{H}_2)_2$  and  $(\text{C}_2\text{H}_2)_3$  are very similar to the transitions of the monomer except for the intensities and the peak widths. The transition position shifts of these clusters, induced by the van der Waals bonding, are within  $10 \text{ cm}^{-1}$  except the  $2_0^1$  transition of dimer and trimer (see data in Table 1). This considerably large shift compared

with other bands could be related to the dipole moment change of the  $\Delta_g$  state induced by  $\nu_2$  vibrational mode. Since all these gerade Rydberg transitions are rotationally unresolved, the observed spectral shifts due to the cluster formation may have relatively large error of  $\pm 1\text{--}2\text{ cm}^{-1}$ . However the intensity ratio of the linear/circular polarized excitation of acetylene clusters indicate that the Rydberg electron has been perturbed by the van der Waals bonding. Fig. 5 gives a typical example. The intensity ratio for the origin of the  $\Delta_g \leftarrow \Sigma_g^+$  transition of  $(\text{C}_2\text{H}_2)_2$  dimer by the linear/circular polarized excitation in Fig. 5 gives a value of  $0.93 \pm 0.04$ . Compared to acetylene monomer (Fig. 4), this value subject a large change. This effect implies that the symmetry of Rydberg orbital has been perturbed by van der Waals bonding.

#### 4.2. Rydberg state stability and geometry of acetylene clusters

The stability of a cluster Rydberg state depends on the coupling between the intermolecular and intramolecular nuclear motion. If such coupling is substantially weak, the Rydberg state of clusters could be stable upon multiphoton excitation. The two-photon transition spectra in Fig. 2 show the stability of  $(\text{C}_2\text{H}_2)_2$  dimer and  $(\text{C}_2\text{H}_2)_3$  trimer Rydberg states. The intensity pattern of these transitions reflect the relative stability of Rydberg vibronic levels. For acetylene dimer  $(\text{C}_2\text{H}_2)_2$ , the transition intensities show that the  $\Delta_g$  electronic state is much more stable than the  $\Sigma_g^+$  electronic state. The relative intensity of the  $\Sigma_g^+$  electronic origin and its vibronic species of the dimer have decreased in comparison to monomer. For both the  $\Delta_g$  and  $\Sigma_g^+$  electronic states of  $(\text{C}_2\text{H}_2)_2$  dimer, the relative intensities for the vibrationally excited states are weaker than their origin, which provides an indication of dissociation caused by the coupling between the intermolecular vibrational modes and the intramolecular vibrational mode. Within these vibrational states of the  $(\text{C}_2\text{H}_2)_2$  dimer, the transition from ground state to the  $\Delta_g$  electronic state with two quanta of bending vibrational excitation (positioned at  $73963\text{ cm}^{-1}$ ) still possess large intensity. This suggests that the vibronic coupling of intermolecular motion and intramolecular motion is relatively weaker in the bending mode than in the other mode ( $\nu_2$  here). This effect must relate to the

geometry of the Rydberg state of this dimer.

The ground state geometry of acetylene dimer has been investigated by several groups using infrared and microwave studies [22–26]. The IR absorption of the acetylene dimer at 600, 2800 [22] and 3279–3285 [23]  $\text{cm}^{-1}$  regions have been interpreted in terms of a planar slipped-parallel  $\text{C}_{2h}$  complex having the axes of the two monomers parallel to one another. Using the radio frequency, microwave, and infrared absorption, Prichard et al. [24] first discovered the T-shaped ( $\text{C}_{2v}$ ) acetylene dimer at the 3271–3274  $\text{cm}^{-1}$  region. Subsequent study of Fraser et al. [25] applying the optothermal molecular-beam color-center laser spectrometer technique, have confirmed both the parallel and perpendicular transitions arising from the  $\text{C}_{2v}$  (T-shaped) complex and the  $\text{C}_{2h}$  complex of the acetylene dimer in the C–H stretching fundamental vibrational mode. The geometry of the acetylene dimer ground state was considered to have a planar T-shaped  $\text{C}_{2v}$  equilibrium geometry with interconversion tunneling between four isoenergetic hydrogen-bonded minima. In such a picture, the parallel and perpendicular bands arise from excitation of the acetylene units parallel and perpendicular to the hydrogen bond. Later study [26] of deuterated acetylene dimers by Fourier-transform microwave spectroscopy proved that this model is valid for the geometry of the ground state. The intensity patterns of the acetylene dimer two-photon Rydberg transition in Fig. 2 support the T-shaped  $\text{C}_{2v}$  equilibrium geometry. The relatively large intensity of the dimer  $\Delta_g$  Rydberg state with two quanta bending vibrational excitation in one monomer shows that the nuclear motion of bending ( $\nu_4$  or  $\nu_5$ ) does not effect the van der Waals bond length and bond angle as much as the  $\text{C}\equiv\text{C}$  stretch. Such results do not favor the parallel  $\text{C}_{2h}$  geometry since the bending motion should strongly couple with the van der Waals vibrational mode, which can lead to fast dissociation. If the acetylene dimer has the T-shaped  $\text{C}_{2v}$  geometry, the bending motion could be relatively isolated from the motion of the van der Waals bond. On the other hand, in the T-shaped  $\text{C}_{2v}$  geometry, the  $\text{C}\equiv\text{C}$  stretching vibration can directly effect the van der Waals bond (hydrogen bond) and result in dissociation. It is interesting to compare the relative intensities of the transition to the  $\Delta_g$  electronic state with two quanta bending vibration excitation in spectra of Fig. 2. The



intensity of this transition in the trimer is much weaker than the corresponding one in the dimer. This is understandable because the trimer is a planar cyclic molecule having a threefold symmetry axis perpendicular to the molecular plane [27]. The bending vibration of intramolecular motion cannot be separated from intermolecular motion, thus the coupling produces the short lifetime for this state. Therefore in the trimer the bending vibration affects the lifetime of Rydberg state in the same fashion as the  $C\equiv C$  stretching. Our results also support the planar cyclic ring structure of  $(C_2H_2)_3$  trimer.

### 4.3. Dynamics of intracluster reaction

Without the pump–probe method for the product detection, it is difficult to discuss the dynamics and the mechanism of the intracluster reactions. However, our results for two-photon Rydberg transitions of acetylene clusters provide indirect information on the dynamics of intracluster reactions.

First of all, there is no detectable signal for the  $C_3H_3^+$  ion in the laser wavelength region used in the present experiment, which is in contrast to the results of Booze and Bear [15], Ono and Ng [13], and Shinohara et al. [8]. The  $C_3H_3^+$  ion has been considered [8] as a product of the dissociative ionization of the acetylene trimer  $(C_2H_2)_3 + h\nu \rightarrow C_3H_3^+ + C_3H_3$ , which indicates that the  $(C_2H_2)_3^+$  ion is not stable. Such dissociative ionization of clusters does not happen in the two-photon resonant Rydberg state ionization here. The adiabatic ionization from the well-defined Rydberg geometry should produce the stable  $(C_2H_2)_3^+$ . On the other hand, the non-adiabatic ionization by the one-photon ionization will produce a broad distribution of the vibrational states of the  $(C_2H_2)_3^+$  ion, which could be unstable. If such is the case, even the Rydberg states can show an unstable character. This probably is why  $C_3H_3^+$  was found in Booze's one-photon threshold ionization experiment with a photon energy well below the ionization potential of acetylene. We believe that the  $(C_2H_2)_3^+$  ion has a stable geometry and can be optically selected through the ionization of a Rydberg intermediate state. One could argue that the  $(C_2H_2)_3^+$  found in our experiment may come from a process involving the ionization of heterogeneous clusters and the

evaporation of Ar atoms  $(C_2H_2)_3 \cdot Ar_m + h\nu \rightarrow (C_2H_2)_3^+ + mAr$ . But these processes are less likely because the evaporation of Ar atoms is much faster in the Rydberg state of clusters than in the ions. For the same reason, the not detectable signal of  $C_4H_2^+$  and  $C_4H_3^+$  in our experiment indicate that the  $(C_2H_2)_2^+$  ion also has a stable geometry.

Secondly we have not observed the strong signals of  $C_2^+$ ,  $C^+$  fragment ions that were resolved in Ashfold's time of flight experiment. These species are believed to be a product of the acetylene monomer. It is interesting to note that there are no detectable  $(C_2H_2)_2^+$  and  $(C_2H_2)_3^+$  ions in their TOF spectra. This effect should relate to the difference of the experimental condition in these two cases. The obvious difference received our attention is the relatively high rotational temperature of their beam and the high acceleration voltage for TOF mass analysis. This implies that the fragmentation of acetylene monomer and cluster could be dependent on rotational temperature. The acetylene dimer ion signal in our case is approximately 15–20 times smaller than the monomer ion. Therefore it is very difficult to detect the cluster ion signal in Ashfold's experiment.

Another interesting aspect of acetylene clusters is whether the  $(C_2H_2)_2^+$  and  $(C_2H_2)_3^+$  retain their character as van der Waals molecular ions or whether they are instead the products of intracluster reactions such as the benzene ion  $C_6H_6^+$ . This question can be addressed in pump–probe experiments. Therefore we only comment briefly here. Since the electronic origin shift of these Rydberg states in clusters is very small, the intracluster reactions for the ground state of cluster ions are less likely. For the vibrationally excited Rydberg states, such possibility could exist. Furthermore, since the van der Waals bond of acetylene clusters are hydrogen-bond like in nature, the heterogeneous acetylene dimer such as the  $C_2H_2 \cdot HCl$  can serve as a good system for the intracluster reaction dynamics. This system is similar to the addition reaction of unsaturated hydrocarbon in organic chemistry.

## 5. Conclusions

Using the two-photon resonant ionization spectroscopy technique, the Rydberg state of acetylene

dimer and trimer clusters has been resolved. The stability of these Rydberg states of acetylene clusters depends on the excitation of vibrational modes. The two-photon resonant ionization spectra of these Rydberg states imply that the geometry of the acetylene dimer and trimer have the planar T-shaped  $C_{2v}$  and planar cyclic symmetry, respectively, and the  $(C_2H_2)_2^+$  and  $(C_2H_2)_3^+$  ions could be stable. The vibrationally resolved Rydberg states of the acetylene cluster can serve for state selection in studying the dynamics of intracuster reactions.

### Acknowledgement

Research was sponsored by the Office of Health and Environmental Research, U.S. Department of Energy under Contract No. DE-AC05-84OR21400 with Martin Marietta Energy Systems, Inc.

### References

- [1] H. Shinohara, J. Chem. Phys. 79 (1983) 1732.
- [2] H. Shinohara, N. Nishi and N. Washida, Chem. Phys. Letters 106 (1984) 302.
- [3] H. Shinohara, N. Nishi and N. Washida, J. Chem. Phys. 83 (1985) 1939.
- [4] N. Washida, H. Shinohara, U. Nagashima and N. Nishi, Chem. Phys. Letters 121 (1985) 223.
- [5] H. Shinohara, N. Nishi and N. Washida, J. Chem. Phys. 84 (1986) 5561.
- [6] H. Shinohara, N. Nishi and N. Washida, Chem. Phys. Letters 153 (1988) 417.
- [7] H. Shinohara and N. Nishi, Chem. Phys. 129 (1989) 149.
- [8] H. Shinohara, H. Sato and N. Washida, J. Phys. Chem. 94 (1990) 6718.
- [9] J.F. Garvey and R.B. Bernstein, J. Phys. Chem. 90 (1986) 3577.
- [10] J.F. Garvey and R.B. Bernstein, Chem. Phys. Letters 126 (1986) 394.
- [11] J.F. Garvey and R.B. Bernstein, J. Am. Chem. Soc. 109 (1987) 1921.
- [12] J.F. Garvey and R.B. Bernstein, Chem. Phys. Letters 143 (1988) 13.
- [13] Y. Ono and C.Y. Ng, J. Chem. Phys. 77 (1982) 2947.
- [14] J.A. Booze and T. Baer, J. Chem. Phys. 96 (1992) 5441.
- [15] J.A. Booze and T. Baer, J. Chem. Phys. 98 (1993) 186.
- [16] K.E. Schriver, A.M. Camarena, M.Y. Hahn, A.J. Pagueia and R.L. Whetten, J. Phys. Chem. 91 (1987) 1786.
- [17] D.C. Dayton and R.E. Miller, Chem. Phys. Letters 143 (1988) 181.
- [18] A.S. Pine and G.T. Fraser, J. Chem. Phys. 89 (1988) 6636.
- [19] M. Takami, Y. Ohshima, S. Yamamoto and Y. Matsumoto, Faraday Discussions Chem. Soc. 86 (1988) 1.
- [20] M.N.R. Ashfold, B. Tutchter, B. Young, Z.K. Jin and S.L. Anderson, J. Chem. Phys. 87 (1987) 5105.
- [21] W.M. McClain and R.A. Harris, Excited states, Vol. 3, ed. E.C. Lim (Academic Press, New York, 1979) ch. 1.
- [22] G.W. Bryant, D.F. Eggers and R.O. Watts, J. Chem. Soc. Faraday Trans. II 84 (1988) 1443; Chem. Phys. Letters 151 (1988) 309.
- [23] R.D. Pendley and G.E. Ewing, J. Chem. Phys. 78 (1983) 3531.
- [24] D.G. Prichard, R.N. Nandi and J.S. Muentner, J. Chem. Phys. 89 (1988) 115.
- [25] G.T. Fraser, R.D. Suenram, F.J. Lovas, A.S. Pine, J.T. Hougen, W.J. Lafferty and J.S. Muentner, J. Chem. Phys. 89 (1988) 6028.
- [26] K. Matsumura, F.J. Lovas and R.D. Suenram, J. Mol. Spectry. 150 (1991) 576.
- [27] D. Prichard, J.S. Muentner and B.J. Howard, Chem. Phys. Letters 135 (1987) 9.